Tunnel-field-effect-transistor based gas-sensor: Introducing gas detection with a quantum-mechanical transducer

Article *in* Applied Physics Letters · January 2013

DOI: 10.1063/1.4775358

CITATIONS
46

READS
387

4 authors:

Deblina Sarkar
Massachusetts Institute of Technology
44 PUBLICATIONS **4,679** CITATIONS

SEE PROFILE

Harald Gossner
Intel
188 PUBLICATIONS **2,108** CITATIONS

SEE PROFILE

Walter Hansch
Universität der Bundeswehr München
120 PUBLICATIONS **1,785** CITATIONS

SEE PROFILE

Kaustav Banerjee
University of California, Santa Barbara
329 PUBLICATIONS **18,777** CITATIONS

SEE PROFILE

AIP | Applied Physics Letters

Tunnel-field-effect-transistor based gas-sensor: Introducing gas detection with a quantum-mechanical transducer

Deblina Sarkar, Harald Gossner, Walter Hansch, and Kaustav Banerjee

Citation: Appl. Phys. Lett. **102**, 023110 (2013); doi: 10.1063/1.4775358
View online: http://dx.doi.org/10.1063/1.4775358
View Table of Contents: http://apl.aip.org/resource/1/APPLAB/v102/i2
Published by the American Institute of Physics.

Tunnel-field-effect-transistor based gas-sensor: Introducing gas detection with a quantum-mechanical transducer

Deblina Sarkar,[1,a)] Harald Gossner,[2] Walter Hansch,[3] and Kaustav Banerjee[1,a)]
[1]*Department of Electrical and Computer Engineering, University of California, Santa Barbara, California 93106, USA*
[2]*Intel Mobile Communications, Am Campeon 1, 85579 Neubiberg, Germany*
[3]*Institute of Physics, Universität der Bundeswehr München, 85577 Neubiberg, Germany*

(Received 27 September 2012; accepted 20 December 2012; published online 17 January 2013)

A gas-sensor based on tunnel-field-effect-transistor (TFET) is proposed that leverages the unique current injection mechanism in the form of quantum-mechanical band-to-band tunneling to achieve substantially improved performance compared to conventional metal-oxide-semiconductor field-effect-transistors (MOSFETs) for detection of gas species under ambient conditions. While nonlocal phonon-assisted tunneling model is used for detailed device simulations, in order to provide better physical insights, analytical formula for sensitivity is derived for both metal as well as organic conducting polymer based sensing elements. Analytical derivations are also presented for capturing the effects of temperature on sensor performance. Combining the developed analytical and numerical models, intricate properties of the sensor such as gate bias dependence of sensitivity, relationship between the required work-function modulation and subthreshold swing, counter-intuitive increase in threshold voltage for MOSFETs and reduction in tunneling probability for TFETs with temperature are explained. It is shown that TFET gas-sensors can not only lead to more than 10 000× increase in sensitivity but also provide design flexibility and immunity against screening of work-function modulation through non-specific gases as well as ensure stable operation under temperature variations. © *2013 American Institute of Physics*. [http://dx.doi.org/10.1063/1.4775358]

Chemical sensors for gases[1–7] are not only indispensable for modern society in order to ensure safety, health, and environmental reservation but can also boost fundamental research in areas like physics of thin films and heterogeneous catalysis. Specially, the gas-sensors based on the work-function modulation of the gate of a field-effect-transistor (FET) is highly attractive due to low power consumption, possibility of integration in microsystems, and ability to detect both chemisorbed and weakly bound physisorbed species at room temperature.[1] In this letter, a gas sensor is proposed that leverages the band-to-band-tunneling current-injection mechanism of Tunnel-FET[8–13] to achieve significantly superior performance under ambient conditions compared to conventional FETs. The results are discussed in terms of two important sensing elements: metal (Pd/Pt) and conducting polymers as the gate material (Fig. 1).

First, we will discuss the gas-sensors with metallic gate as sensing element. Thick, continuous metallic gate can be used to sense hydrogen.[2,3] The transduction mechanism involves dissociation and adsorption of hydrogen molecules at the metal surface and thereby diffusion of some atomic hydrogen into metal, which form dipoles at the interface changing the gate work function (WF_G) (Fig. 2(a)). This process depends on the flux of gas Ψ given by $\Psi = P/\sqrt{2\pi m_g K_B T}$, heat of adsorption at surface ΔH_s, and interface ΔH_i, which follows the Tempkin Isotherm as $\Delta H_i = \Delta H_{i0}(1 - \alpha\xi_i)$, where $\alpha = q\mu N_i/(\varepsilon \Delta H_{i0})$, P: gas pressure, m_g: gas molecular mass, K_B: Boltzmann constant, T: temperature, ΔH_{i0}: initial heat of adsorption, ξ_i: interface coverage of hydrogen defined as the ratio of hydrogen concentration at interface to the total concentration of hydrogen adsorption sites at interface and is a function of hydrogen gas flux,[14] N_i: total concentration of hydrogen adsorption sites at interface, q: elementary charge of an electron, μ: effective dipole constant, and ε: permittivity. The change in work function is given by[3]

$$\Delta WF_G = -(\xi_i N_i \mu)/\varepsilon. \tag{1}$$

Fig. 2(b) shows the ΔWF_G of metal gate as a function of hydrogen gas pressure.

The ΔWF_G can be employed to bend the bands in a tunnel-field-effect-transistor (TFET) and hence modulate its current. A non-local 2D model based on self-consistent solutions of Poisson's and Schrodinger's equations including the effect of phonons, is used for detailed device simulations. At the same time, in order to provide better physical insights, an analytical expression for sensitivity (S_n) is derived using simplified 1D model. The 1D Poisson's equation (Eq. (2)) is solved to obtain the potential in the channel assuming high source doping and hence neglecting band bending in source.

$$\frac{d^2\varphi_i(x)}{dx^2} - \frac{\varphi_i(x) + V_G - WF_G + WF_S}{\lambda^2} = 0. \tag{2}$$

Here, φ_i: potential at semiconductor-oxide interface, WF_S: semiconductor work function, V_G: gate voltage, and λ: natural length scale.[15] Then, calculating tunneling probability using the WKB approximation and the two-band approximation,[13] the band-to-band-tunneling current (I_{BTBT}) is derived using Landauer's formula[16] following the procedure described in Ref. 17

a)Authors to whom correspondence should be addressed. Electronic addresses: deblina@ece.ucsb.edu and kaustav@ece.ucsb.edu.

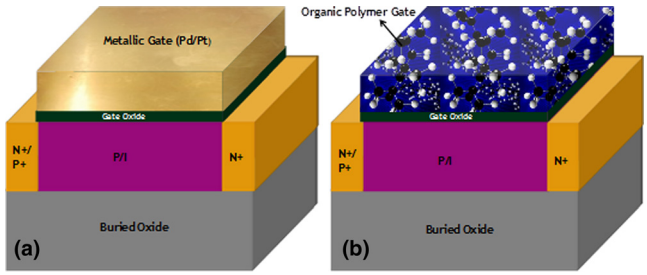

FIG. 1. The schematic diagram of a field-effect-transistor gas-sensor based on silicon-on-insulator (SOI) structure with (a) metallic gate and (b) organic conducting polymer gate as the sensing element. For conventional n-type MOSFET based sensor, the doping in source, channel, and drain are N+, P, and N+, respectively, while for that based on n-type TFET, the sequence is P+, I, and N+, respectively. Continuous Pd and Pt film is explored for metallic gates, while polyaniline and polypyrrole are discussed for polymer gates. Semiconductor material is taken to be silicon. Note that we use the term MOSFETs generically to specify conventional FETs even in case of a polymer gate. For all simulations the channel length is taken to be 50 nm, effective gate oxide thickness is 0.5 nm and thickness of SOI is 5 nm for both MOSFET and TFET.

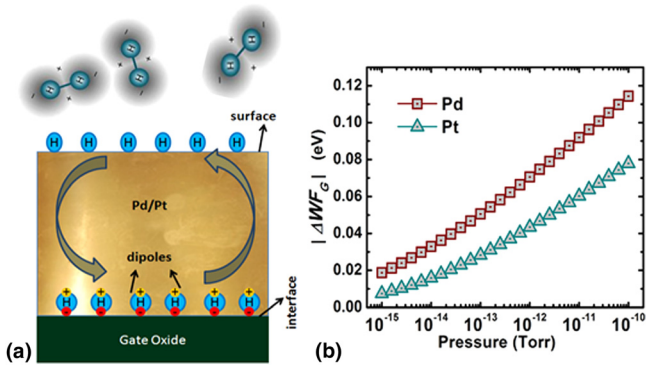

FIG. 2. (a) The schematic diagram of dipoles at the interface of metal and oxide layer. (b) Change in work-function of Pd and Pt metal gate as a function of hydrogen gas pressure. Interface concentration of hydrogen sites and sticking coefficient is lower for Pt[5] compared to those for Pd leading to lower values of ΔWF_G for same hydrogen pressure. Note that ΔWF_G is negative and absolute values have been plotted here.

$$I_{BTBT}(WF_G) = 2q^2/h \exp(-\pi\sqrt{q}m^{*1/2}E_G{}^{3/2}\lambda/(\sqrt{2}\hbar(2(V_G - WF_G + WF_S) - E_G))) \int_0^{V_G - WF_G + WF_S - E_G} (f_S - f_D)\, dE\,. \quad (3)$$

Here, h: Plank's constant, m^*: carrier effective mass, E_G: bandgap of semiconductor, f_S: Fermi function at source, and f_D: Fermi function at drain. WF_G can be written as the sum of initial work-function (WF_{G0}) and change in work function. Sensitivity (S_n) is defined as the ratio of change in current after gas adsorption to the initial current before gas adsorption and is given by

$$S_n = \{I_{BTBT}((V_G - WF_{G0}) - \Delta WF_G) - I_{BTBT}(V_G - WF_{G0})\}/I_{BTBT}(V_G - WF_{G0}). \quad (4)$$

Using Eqs. (1), (3), and (4), S_n of TFET gas sensor is derived setting source Fermi function to 1 and drain Fermi function to 0 and is given by

$$S_n = \left\{\left[\exp\left(\frac{\pi\sqrt{2q}m^{*1/2}E_G{}^{3/2}\lambda(\xi_i N_i\mu)/\varepsilon}{\hbar(2(V_G - WF_{G0} + WF_S) - E_G)(2(V_G - WF_{G0} + WF_S) + 2(\xi_i N_i\mu)/\varepsilon - E_G)}\right)\right]\left(1 + \frac{(\xi_i N_i\mu)/\varepsilon}{V_G - WF_{G0} + WF_S - E_G}\right)\right\} - 1. \quad (5)$$

In Figs. 3(a) and 3(b), S_n is plotted as a function of the gate bias and the gas pressure for metal-oxide-semiconductor field-effect-transistors (MOSFETs) and TFET, respectively. It is observed that for both, maximum S_n is obtained in the subthreshold region. This can be understood since the highest effect of gate occurs in the subthreshold region. In MOSFETs, the subthreshold swing (SS) is limited by the *Boltzmann Tyranny effect* to $[K_BT/q \ln(10)]$, which also puts severe limitations on the achievable sensitivity. TFETs overcome this limitation due to the *Fermi-tail cutting* by the

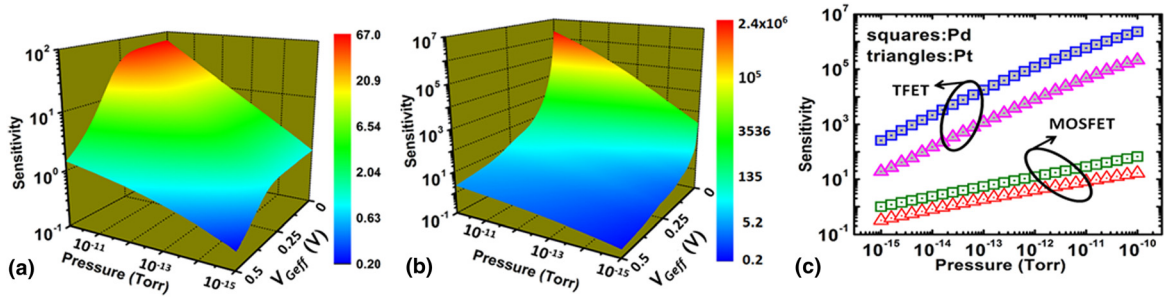

FIG. 3. Color-map showing the importance of gate bias and operation regime of FET on the performance of (a) MOSFET and (b) TFET based gas-sensors. Pd is used as a gate material for both cases. For convenience of plotting and understanding, the effective gate voltage is offset from the actual gate voltage such that for MOSFET, V_{Geff} is taken to be 0 at 0.35 eV lower than the threshold voltage. For TFET, $V_{Geff} = 0$ where the SS is minimum. At any value of gas pressure, sensitivity of MOSFET gas-sensor remains almost constant for lower values of V_{Geff} due to the almost constant SS of MOSFET. However, with increase in V_{Geff}, effect of gate decreases as MOS crosses the subthreshold region and hence the sensitivity degrades. For TFET gas-sensor, sensitivity keeps on increasing as V_{Geff} is decreased due to the improvement in SS. The average SS of the TFET over 0.1V of gate voltage near $V_{Geff} = 0$ is 13 mV/dec. By effective tuning of gate bias, sufficient improvement in sensitivity can be achieved through TFET gas-sensor compared to that of MOSFET gas-sensors. (c) Comparison of sensitivity of MOSFET and TFET gas-sensors, both biased at $V_{Geff} = 0$. Sensitivity of both MOSFET and TFET are calculated through self-consistent numerical simulations.

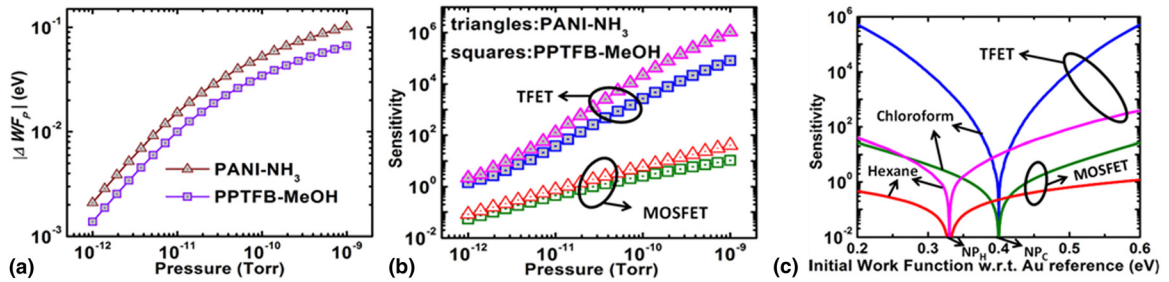

FIG. 4. (a) Change in work-function of polymer gate and (b) sensitivity comparison of TFET and MOSFET sensors as a function of gas pressure. Results are shown for sensing of ammonia with PANI and methanol with PPTFB. The effect of non-specific background gases is captured through the term $\sum k_i P_i$ in Eq. (6) and is taken to be 10^{-11} in both cases. (c) Sensitivity of MOSFET and TFET gas-sensors with polymer gate based on polypyrrole and p-poly-phenylene for sensing hexane and chloroform as a function of initial work function of the polymer (with respect to the work function of the Au reference grid). TFET gas-sensors lead to much higher sensitivity compared to those based on MOSFETs even in the region near the NP. The neutrality points are marked in the figure as NP_H and NP_C for hexane and chloroform, respectively. Sensitivity of both MOSFET and TFET are calculated through self-consistent numerical simulations.

bandgap and hence can lead to significantly higher S_n for gas sensing as shown in Fig. 3(c). TFETs can also exhibit high S_n for the detection of charged biomolecules.[17–19]

Now, we will focus on organic conducting polymer gate as sensing element. Organic conducting polymers can be used to obtain selective detection of specific target gas molecules. The gas molecules form a charge transfer complex with the polymer matrix through the exchange of a fractional charge δ.[6,7] Depending on the sign (positive/negative) of δ, the gas molecules behave as a secondary dopant (acceptor/donor) and change the Fermi level and hence the bulk component of work function of the polymer (WF_P). ΔWF_P is given by[7]

$$\Delta WF_P = K_B T/2\delta \ln\left(P/\sum_i k_i P_i + 1\right), \tag{6}$$

where $\delta = \gamma(E_F - \chi_g)$, E_F: Fermi level of polymer, χ_g: Mulliken electro-negativity coefficient of gas, P_i: pressure of background non-specific gases, k_i: selectivity coefficients, WF_{P0}: work function before gas absorption, γ: proportionality constant.[6] Using Eqs. (3), (4), and (6), analytical formula for sensitivity of TFET gas-sensor is derived as

$$S_n = \left\{\left[\exp\left(\frac{\pi\sqrt{2q}\, m^{*1/2} E_G^{3/2} \lambda |\Delta WF_P|}{\hbar(2(V_G - WF_{PS0}) - E_G)(2(V_G - WF_{PS0}) + 2|\Delta WF_P| - E_G)}\right)\right]\left(1 + \frac{|\Delta WF_P|}{V_G - WF_{PS0} - E_G}\right)\right\} - 1\,, \tag{7}$$

where ΔWF_{PS0} is the initial work function difference between the polymer and semiconductor. From Figs. 4(a) and 4(b), it is clear that TFETs provide substantial increase in S_n compared to conventional FETs as shown for detection of NH_3 and CH_3OH (MeOH) with polyaniline (PANI) and poly- pyrrole-tetrafluoroborate (PPTFB), respectively. The change in WF of polymers depends on its initial WF (WF_{P0}), which varies with varying growth conditions.[6] If E_F equals χ_g, no charge transfer takes place and $\Delta WF_P = 0$. We call this point the neutrality point (NP). $|\Delta WF_P|$ increases as WF_{P0} moves away from NP. For MOSFETs, reasonable S_n is obtained only further away from NP (Fig. 4(c)) and thus requires high control of polymer growth conditions to achieve specific WF_{P0}. In TFETs, high S_n can be achieved even in regions near NP (Fig. 4(c)), thus providing flexibility and facilitating ease of polymer growth process.

In Fig. 5, S_n is plotted as a function of SS taking an example each from metallic gate as well as polymer gate as sensing element. It is observed that in both cases S_n increases substantially with the decrease in SS. This figure has important technological implications and shows that extremely high S_n can be achieved through implementation of low SS devices like TFET in gas-sensor technology.

To be applicable for practical applications, a sensor should possess high efficiency under ambient conditions in the presence of non-specific background gases. In the case of polymer film, it is clear from Eq. (6) that increase in $\sum k_i P_i$ term (which represents the effect of background gases) decreases ΔWF_P. In the case of metallic gate, the presence of oxygen in air sufficiently reduces the surface and interface coverage of hydrogen (Fig. 6(a)) and hence the $|\Delta WF_G|$ (Fig. 6(b)) due to water formation and subsequent desorption

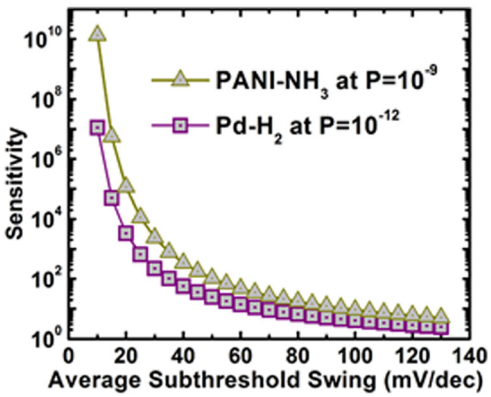

FIG. 5. Sensitivity as a function of average subthreshold swing for both metallic gate (Pd for sensing hydrogen at pressure of 10^{-9} Torr) as well as polymer gate (PANI for sensing ammonia at pressure of 10^{-12} Torr) as the sensing element.

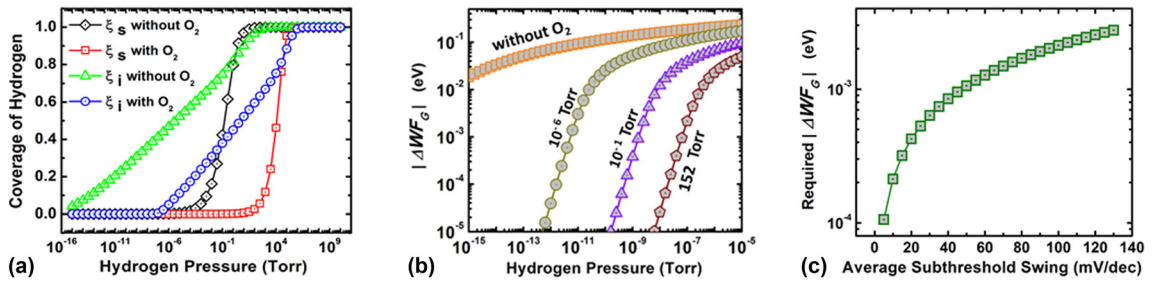

FIG. 6. (a) The surface (ξ_s) and interface (ξ_i) coverage of hydrogen in Pd without and in the presence of oxygen (152 Torr) as a function of hydrogen pressure. (b) Effect of varying oxygen pressures (10^{-6}–152 Torr) on $|\Delta WF_G|$. ξ_s, ξ_i and $|\Delta WF_G|$ decrease in the presence of oxygen. (c) The change in gate work function that is required to obtain a desired sensitivity (here, the desired value is taken to be 0.05) is plotted as a function of the average subthreshold swing. The required $|\Delta WF_G|$ decreases strongly with decrease in *SS*. Hence, the same sensitivity can be achieved at much lower values of $|\Delta WF_G|$ for low *SS* devices like TFET.

reactions.[4] From Fig. 6(c), it is observed that if the *SS* is reduced, the $|\Delta WF_G|$ required to achieve a desired sensitivity can be more than an order lower. Hence, TFETs with low *SS* can be highly beneficial in detection of target gas molecules under atmospheric conditions where the presence of non-specific gases screen the change in gate work function.

For stable operation, the influence of temperature (T) variations on the sensor performance should be minimal. T affects the sensor performance by influencing (i) interaction between the gas and sensing element and (ii) properties of semiconductor. Here, the effect of T is discussed taking the metallic gate as an example and it is seen that the increase in T leads to the reduction in hydrogen coverage and hence the $|\Delta WF_G|$ (Fig. 7(a)). We define the T affectability (A_T) as

$$A_T = \{I(T+\Delta T) - I(T)\}/I(T)\,. \tag{8}$$

Analytical equations of T affectability are derived for both MOSFET ($A_{T\text{-}MOS}$) and TFET ($A_{T\text{-}TFET}$) based gas-sensors and are given by

$$A_{T-MOS} = \left\{\exp\left(-\frac{-(N_i\mu\Delta\xi_i)/\varepsilon + \Delta\varphi_b - \Delta E_G/2 - \Delta EA}{K_B(T+\Delta T)/q}\right)\exp\left(-\frac{\Delta T/T(V_G - WF_G - \varphi_b + E_G/2 + EA - qNat_{Si}/C_{ox})}{K_B(T+\Delta T)/q}\right)\right\} - 1\,, \tag{9}$$

$$A_{T-TFET}(WF_G) = \exp(-\pi\sqrt{q}m^{*\,1/2}\lambda/\sqrt{2}\hbar \times \Delta Fnc\,(T)) - 1, \tag{10a}$$

$$Fnc\,(T) = E_G(T)^{3/2}/(2(V_G - WF_G(T) + WF_S(T)) - E_G(T))\,. \tag{10b}$$

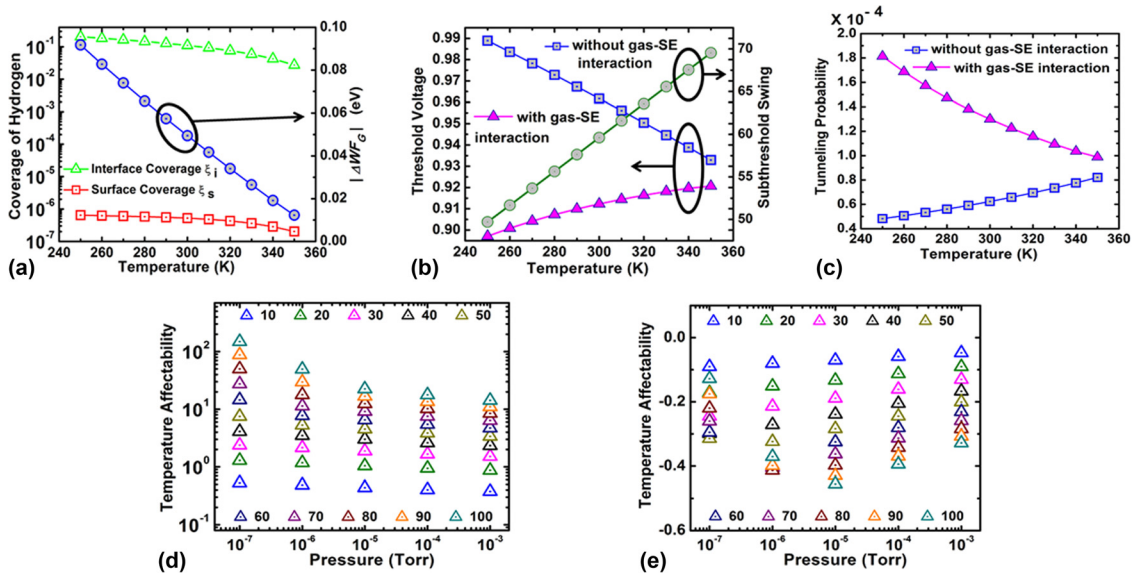

FIG. 7. (a) Effect of temperature (T) variations on gas-sensor performance. $|\Delta WF_G|$ decreases with T due to decrease in the surface (ξ_s) and interface (ξ_i) coverage of hydrogen. (b) $A_{T\text{-}MOS}$ is dominated by change in threshold voltage (V_{th}) through modification in interaction term between the gas and sensing element (SE) ($\mu N_i\xi_i/\varepsilon$) and semiconductor properties (φ_b, E_G, and EA) and the change in *SS*. (c) $A_{T\text{-}TFET}$ is dominated by change in tunneling probability through modification of WF_G (due to gas-SE interaction) and semiconductor bandgap. A_T is plotted for (d) MOSFET and (e) TFET with $T = 250$ K and ΔT varying from 10 K to 100 K. A_T is positive in MOSFET (current increases with T) due to the increase in *SS* compensated to some extent due to increase in increase in V_{th}. A_T is negative in TFET due to the decrease in tunneling probability with T. Overall $A_{T\text{-}TFET}$ is much smaller than $A_{T\text{-}MOSFET}$. Note, that the isothermal point[20] (*IP*) of MOSFET occurs in the super-threshold region, which will lead to degraded sensitivity and *IP* will vary with gas adsorption. Hence, a TFET based gas-sensor can offer much more stable operation under T variations compared to that based on MOSFETs.

Here, φ_b: energy difference between the Fermi level of semiconductor and its intrinsic Fermi level, *EA*: electron affinity of semiconductor, *Na*: channel doping concentration, t_{si}: silicon thickness, and C_{ox}: gate capacitance. *T* influence MOSFET subthreshold current mainly through change in the threshold voltage (V_{th}) and *SS*. It is well known that in MOSFETs, V_{th} decreases as *T* increases. However, the MOSFET gas-sensor exhibits a counter-intuitive opposite trend (Fig. 7(b)). This behavior can be explained by the increase in WF_G ($=WF_{G0} - |\Delta WF_G|$) with *T* due to the decrease in gas adsorption and hence $|\Delta WF_G|$. The *SS* of MOSFET increases linearly with *T*. For a silicon TFET for digital applications, it has been experimentally demonstrated[9] that dominant factor through which *T* influences the current is through increase in the tunneling probability (P_{BTBT}) due to the decrease in bandgap (E_G) (phonon emission is nearly independent of *T*). For TFET gas-sensor, the situation is different and the factor through which *T* dominantly affects the current is given by *Fnc(T)* (Eq. (10b)). It is observed that the increase in P_{BTBT} due to decrease in E_G is offset by the increase in WF_G term that occurs in the denominator of *Fnc(T)*. Hence, P_{BTBT} of TFET gas sensor decreases with *T* (Fig. 7(c)). From Figs. 7(d) and 7(e), it is clear that the TFET has substantially lower A_T than that of MOSFETs and hence it is much less vulnerable to *T* variations.

A gas-sensor based on tunnel-field-effect-transistor is proposed and its characteristics are analyzed through numerical as well as analytical modeling. The TFETs due to their ability to obtain very low subthreshold swing are highly advantageous compared to MOSFETs for gas sensing under ambient conditions. For practical applications, it is necessary that low values of subthreshold swing are obtained at measurable current levels. Till now, the lowest experimentally reported subthreshold swing at a measurable current level is 30 mV/decade in Si nanowire based TFETs.[10,11] Further improvement in electrostatic control of gate and introduction of low-bandgap materials can lead to even better performance. Thus, while TFETs have mainly evolved with an aim of reducing the power consumption in digital electronics, it is shown here that, it also holds great promise in a completely diverse arena of gas-sensor technology.

This work was supported by the U.S. National Science Foundation, Grant No. CCF-1162633.

[1]C. Senft, P. Iskra, I. Eisele, W. Hansch, *Chemical Sensors: Comprehensive Sensor Technologies* (Momentum, 2011), Chap. 4.
[2]I. Lundstrom, S. Shivaraman, C. Svensson, and L. Lundkvist, Appl. Phys. Lett. **26**, 55 (1975).
[3]J. Fogelberg, M. Eriksson, H. Dannetun, and L.-G. Petemona, J. Appl. Phys. **78**, 988 (1995).
[4]J. Fogelberg and L.-G. Petemona, Surf. Sci. **350**, 91 (1996).
[5]A. Salomonsson, M. Eriksson, and H. Dannetun, J. Appl. Phys. **98**, 014505 (2005).
[6]J. Janata and M. Josowicz, Acc. Chem. Res. **31**, 241 (1998).
[7]J. Janata, Collect. Czech. Chem. Commun. **74**, 1623 (2009).
[8]P. F. Wang, K. Hilsenbeck, T. Nirschl, M. Oswald, C. Stepper, M. Weis, D. Schmitt-Landsiedel, and W. Hansch, Solid-State Electron. **48**, 2281 (2004).
[9]M. Born, K. K. Bhuwalka, M. Schindler, U. Abelein, M. Schmidt, T. Sulima, and I. Eisele, in *Proceedings of the International Conference on Microelectronics* (2006), p. 124.
[10]R. Gandhi, Z. Chen, N. Singh, K. Banerjee, and S. Lee, IEEE Electron Device Lett. **32**, 437 (2011).
[11]R. Gandhi, Z. Chen, N. Singh, K. Banerjee, and S. Lee, IEEE Electron Device Lett. **32**, 1504 (2011).
[12]D. Sarkar and K. Banerjee, Appl. Phys. Lett. **99**, 133116 (2011).
[13]D. Sarkar, M. Krall, and K. Banerjee, Appl. Phys. Lett. **97**, 263109 (2010).
[14]L.-G. Ekedahl, M. Eriksson, and I. Lundstrom, Acc. Chem. Res. **31**, 249 (1998).
[15]R.-H. Yan, A. Ourmazd, and K. F. Lee, IEEE Trans. Electron Devices **39**, 1704 (1992).
[16]S. Datta, *ECE 659 Quantum Transport: Atom to Transistor* (NanoHub, 2009); available at https://nanohub.org/resources/6172.
[17]D. Sarkar and K. Banerjee, Appl. Phys. Lett. **100**, 143108 (2012).
[18]D. Sarkar and K. Banerjee, in *Proceedings of the Device Research Conference* (2012), p. 83, see http://ieeexplore.ieee.org/xpls/abs_all.jsp?arnumber=6256950&tag=1.
[19]A. Moscatelli, P. Rodgers, M. Segal, and O. Vaughan, Nat. Nanotechnol. **7**, 275 (2012).
[20]M. Burgmair, H.-P. Frerichs, M. Zimmer, M. Lehmann, and I. Eisele, Sens. Actuators B **95**, 183 (2003).